Measurement of Velocity Fields in Ball Mills

by L.-S. Kung and J.-C. Samin

ABSTRACT—This paper describes a computer vision technique used in measuring the velocity field related to the motion of balls in a ball mill. A camera combined with two color flashes facing an experimental ball mill is used to take pairs of pictures by triggering the flashes in sequence with a time interval Δt. In order to ensure consistency, the pictures are of different colors and in a single frame. The ball positions in each image are detected by image-processing techniques, and the velocity is then the displacement of each ball between two successive images divided by Δt. The measurement error is estimated by measuring the displacements from a pair of images when the balls remain stationary.

Introduction

Grinding is obtained via balls moving in a ball mill; many phenomena, therefore, can be investigated by observing the motion of the balls (i.e., the effect of a lift bar, the crushing mechanism and the sliding of the mill load). Conclusions from observation and empirical models are still widely used by designers.

Researches have been conducted either theoretically or experimentally in checking the motion of a single ball,[5,6,9] but the results are not sufficient to evaluate the performance of an entire mill. For analyzing the entire mill, there is a computer simulation program which tracks the motion of balls in large-diameter ball mills.[7] The simulation gives the force distribution, fall-height distribution and energy distribution of the balls, but the theoretical simulation model has not yet been validated.

This paper presents a means by which to measure the velocities of all the balls in the mill in order to have a quantitative idea of ball motion as a preliminary step in determining the empirical model of ball behavior. In addition, the result provides the velocity distribution of the balls.

There are various techniques for measuring the velocity. In our case, it is difficult to put sensors in a ball mill or inside the balls.[3] Therefore, a computer vision technique is proposed in order to measure the velocities of a large quantity of balls.

Measuring the velocity of moving objects by computer vision techniques can be done via two distinct approaches:[1] (1) feature-based approach and (2) optical-flow-based approach. The feature-based approach is chosen because balls, the moving objects, are simple in shape and relatively easier to identify from a frozen image than from an optical flow image. Because of the large number of moving objects, the difficulties of this approach lie in the procedures to find the interimage relations and to match the balls between images.

L.-S. Kung is a Doctoral Student and J.-C. Samin is a Professor, Unité Production et Machines (PRM), Université Catholique de Louvain, Institut Stévin, Place du Levant 2, B-1348 Louvain-la-Neuve, Belgium.

Similar to the general steps of the feature-based approach,[2] our task is categorized into four major steps (see Fig. 1):

1. Acquire two successive images I_t and $I_t + \Delta t$ for known Δt
2. Identify ball positions in each image
3. Match the corresponding balls between I_t and $I_t + \Delta t$
4. Measure the displacement Δd of each ball between the image pair.

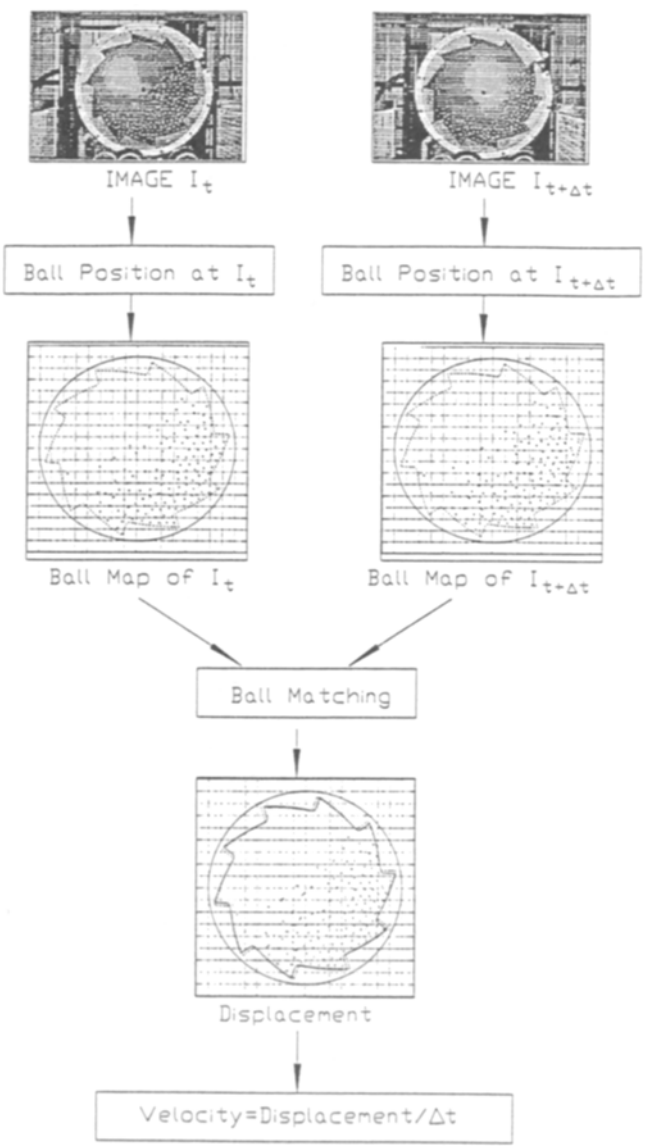

Figure 1: Method for measuring the velocity field

The velocity v of each ball is then

$$v = \frac{\Delta d}{\Delta t} \tag{1}$$

In the first step, two frozen images are required. A CCD camera is not able to take frozen images due to the lag of photo sensors, nor is a video camera because of the fixed rate of image frames and low resolution. So an ordinary camera was used to take frozen images by flash light; the images were then transferred into digital form via a CCD camera. In order to take two images in a very short time interval and maintain the best consistency, I_t and $I_{t+\Delta t}$ were taken in different colors and then put into the same frame of film. The drawback of using an ordinary camera is the film deformation.

In the second step, an image-processing technique is used to extract the balls and determine their positions. This technique uses the difference in brightness between the balls and the background, the balls being the bright spots and the background being the dark area. Any rotation of the individual balls is not detectable by this procedure.

In the third step, the procedure of matching is dependent on the complexity of the image. The image was set up using a specially designed experimental mill and image acquisition devices; the image therefore is simple and hence the matching procedure is as well. After the corresponding ball pairs have been found in the matching process, the displacement of each ball, in the last step, can be calculated via the difference of corresponding ball centers.

In the following, the matching rule will first be explained, since the apparatus and the procedures are designed according to this rule. In the second section the matching rule is described. In the third section the apparatus is described. In the fourth section we discuss the image-processing algorithms for finding ball positions and matching balls between two images. The measurement results and the measurement errors are reported in the fifth section.

Rule of Matching

Matching an identical ball between images is not easy, since all the balls have the same shape, same size and approximately the same brightness. But when the balls are well separated and the corresponding balls are not far away from each other, they can be matched without great effort. In order to devote less effort to the matching process, an experimental ball mill has been built that allows only a single layer of balls. This model assumes that the effects between layers of balls are negligible.

For a single layer of balls, the rule is set up by considering the balls as two-dimensional disks which cannot overlap. If all the balls have the same radius r_b, and the magnitude of displacement Δd of all balls between successive images is less than r_b,

$$\Delta d < r_b \tag{2}$$

then the corresponding ball centers will always be located inside the disk of its radius. Thus the matching operation is simply to find the nearest ball in the image pairs.

The constraint of eq (2) is met by controlling the time difference Δt between images I_t and $I_{t+\Delta t}$. For different mill velocities, the maximum magnitude of Δd should be kept below the ball radius by using a suitable Δt. In other words, the maximum speed of the ball can be used as the criterion for setting Δt.

By observation, the ball with highest speed is always a free-flying ball. Since the flying balls are well separated and they seldom lead to mistakes in matching, the ball speed in a high-density area is used as the criterion. The high-density region is near the bottom of mill, and the balls touching the liner always have the highest speed. The ball speed for setting Δt can thus be roughly calculated as

$$\frac{\Delta d}{\Delta t} \approx \pi N D_n \tag{3}$$

where N is the number of rotations per second of the mill and D_n is the average diameter of the liner. In eq (3), the ball slip on the liner and the ball radius are neglected. The average diameter of the liner is used because its profile is not a cylinder with uniform diameter. From eq (2), Δt is expressed as

$$\Delta t < \frac{r_b}{\pi N D_n} \tag{4}$$

Equation 4 is only a reference rule. The value Δt also depends on the profile of the liner, percentage of filling and the mill speed. For example, if the balls are separated due to high mill velocity and low filling, the Δt could be larger. The calculation of eq (4) was used as a reference, and the value of Δt was chosen by experiment.

Image Acquisition

This section describes the objective of obtaining an image containing the balls which are distinct from the background for ease of identification, and the balls which are well separated for ease of matching. This goal is achieved by a specially designed experimental ball mill and specific photographic equipment.

Experimental Ball Mill

The experimental mill, as shown in Fig. 2(a), is a reduced model with a transparent glass window. The internal diameter of the drum D_m is 0.8 m. The liner is fixed inside the drum to hold the balls and transfers energy to the balls as the drum rotates. A ring is used to fix the glass shield on the drum, and there are fake balls painted on the fixing ring. The purpose of the fake balls will be described in the next section.

In order to comply with the rule of matching, the mill length allows only one layer of balls. The balls can move freely in the radial direction but not in the axial direction.

The mill speed S is adjustable so that one can observe the ball motion under different operating conditions. It is defined as

$$S = \frac{N}{N_c} \tag{5}$$

where N is the number of rotations per second and N_c is the critical mill speed, that is, the speed at which all balls are completely centrifugated.

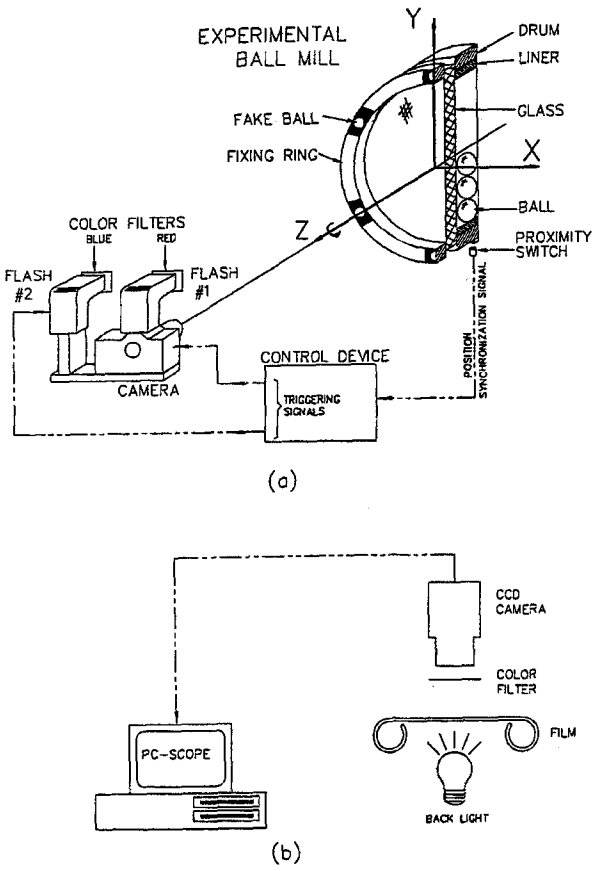

Fig. 2—Apparatus for image acquisition. (a) The experimental ball mill and the image-taking equipment. (b) Equipment for digitizing the images

Photographic Equipment

As shown in Fig. 2(a), a camera, two flashes and a "control device" are used to take photographs. There are color filters for each flash, and the colors are complementary (e.g., blue and red).

The control device triggers the camera shutter and the flashes in a predetermined sequence. A proximity switch is mounted near the drum, and its actuator is mounted on the drum. Whenever the actuator passes the switch, the latter is actuated and sends a switching signal to the control device for synchronizing the position of the mill. The synchronization signal allows all the photographs to be taken at the same mill position, which is useful in comparing the velocity fields with different liner profiles.

The sequence of the control device is started by a "fire" signal given by the operator. The device then waits for the synchronization signal. As soon as a synchronization signal comes in, the control device sends out a triggering signal to the camera shutter. After the first flash, the control device sends a triggering signal to the second flash with a time difference Δt. When the photographs are taken with flash light, the balls' motions are frozen. If we neglect the time delay of the flash light after the triggering signal, the time difference of two images is equal to Δt.

The control device is an in-house electronic board, and the precision of Δt setting is within 1 μs.

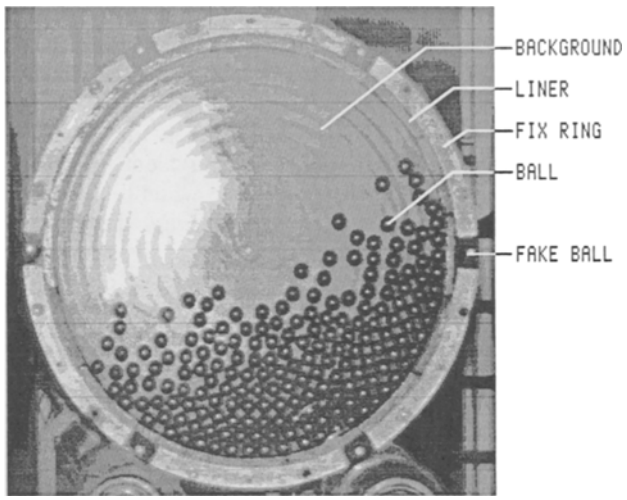

Fig. 3—A digital image

Digital Images

Photographs were taken using color slides, and each frame of slides contains two images in different colors. A CCD camera and the same color filters for the flashes are used to separate images and transfer them to digital form [Fig. 2(b)]. From each frame of slides, we receive two black and white images by changing only the color filters without moving the CCD camera or the film, so there is almost no positional discrepancy between images.

The resolution of digital images is 512 × 512 pixel, and each pixel has a gray level from 0 (black) to 255 (white). A commercial image-processing software, PC-SCOPE,[8] is used.

Image Analysis

A picture of the ball mill, shown in Fig. 3, shows the fixing ring, liner, balls and background. The drum, which is behind the fixing ring, cannot be seen on this view.

There are fake balls painted on the fix ring. The fake balls are used for finding the mill center, the mill angle and the mill speed. Theoretically, the velocities of all fake balls should be equal and tangent to the rotation center; therefore, the accuracy of the measurement can be verified at a glance by examining the fake balls.

In the following, the procedures for detecting the positions of both fake balls and real balls by image-processing techniques, and then the matching process of two successive images, will be described. The procedures are developed in C language integrated with PC-SCOPE subroutines.[8]

Fake Ball

There are six fake balls equally distributed around the drum. Only five are used because one of them is sometimes hidden or in the dark.

The fake balls are the white solid disks painted on the black background. Because of the good contrast, they can

be found by a threshold gray level. The threshold value for each fake ball is different even in the same image due to the uneven lighting conditions. In order to find a fake ball, the threshold is adjusted according to the total number of pixels whose gray levels are greater than the threshold, where the total number of pixels is equivalent to the area of the white disk. When the area of the white disk is equal to the known ball area, the threshold is regarded as the best value.

In the procedure, the fake balls are identified one by one and manually. For each of them, the user is invited to pick an initial point inside the white disk and then the program will carry out the following:

1. Start from a default threshold gray level.
2. Around the initial point, check the total number of pixels with gray level greater (brighter) than the threshold.
3. If the total number of pixels is larger than the area of a fake ball, increase the threshold; otherwise, decrease the threshold.
4. Repeat step 2 until the total number of pixels is in an acceptable range.
5. Calculate the center of mass of these pixels as the position of the fake ball.

The positions of the five fake balls are used as reference points for the mill position. A circle is fitted to these five ball centers using least square fitting. The scale factor of the image is then the ratio between the circle radius and the real measurement. The center of the fitted circle is the center of the mill. When the liner shape is not a cylinder, the mill angle is defined using the a priori knowledge of the shift angle between the fake balls and the liner.

Real Ball

About 190 balls, 30 mm in diameter, fill the experimental mill to 30-percent capacity. Each ball in the image is characterized by a bright spot (high gray-level value) and the gray level decreasing gradually around it. The ball and its position are found by detecting the bright spot in the image. In order to enhance the bright spot relative to the background, a Laplacian operator (appendix), which is a standard process in PC-SCOPE,[8] is used. After the enhancement, the image shows a good contrast between the balls and the background. A simple threshold gray level produces the bilevel image as shown in Fig. 4, leaving only the islands of white pixels representing the balls. The program then performs the following:

1. Scans the image to find all the islands which represent the bright spots of the balls; and
2. Calculates the center of mass of each island as the ball position in the image.

The procedures described above are performed only on the area of the image which is covered by the mill in order to save processing time. As a result, over 80 percent of balls are always correctly located. The percentage can be higher, sometimes 100 percent, if the image has good quality and the threshold gray level is well adapted. The missed balls result from a noisy background and bad ball surface. The noisy background is due mainly to the reflection of flash light by the glass and the end plate of the drum.

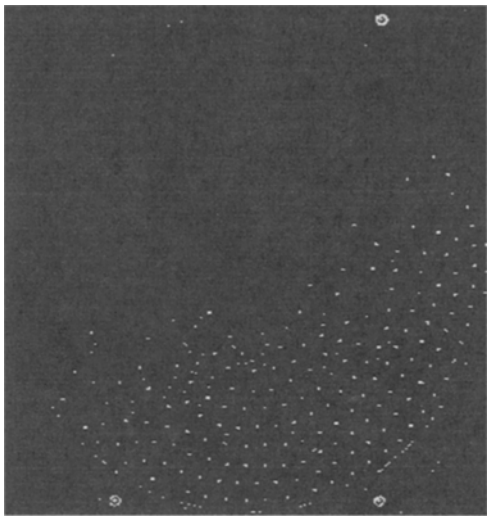

Fig. 4—Bi-level image after enhancement by the Laplacian operator

After the automatic procedures, the user is then requested to edit and confirm the result manually. Editing is done by using the mouse. In the editing mode, a ball can be deleted or added by clicking the mouse when the cursor is in the desired position. It is unavoidable, sometimes, that a few balls are difficult to find during the confirmation by the user. They can, however, be detected and corrected during the matching process.

Correction of the Ball Position

The ball positions in the image are not yet the *true* positions. This is not only because the camera, the flashes and the balls are not aligned, but also because the refraction of the glass shield distorts the image. Furthermore, the different depths of true balls and fake balls in the experimental mill need also to be taken into consideration.

By ray-tracing rules as shown in Fig. 5, the position of the bright spot $\hat{y}$ can be found as measured in the plane containing the painted fake balls. This plane is defined as the *image plane* because all the measurements from the image are made in this plane. The true ball position y should be measured from the ball center instead of the bright spot.

In calculating the true position, y, it is assumed that the ball is perfectly spherical and always contacting the glass, the flashes are point light sources and the plane containing the camera focus point and the two flashes is perpendicular to the rotation axis of mill. The y-z plane is used as an example to explain how to calculate the true position y from the position of a bright spot $\hat{y}$. The same procedure of calculation can be applied to the x-z plane.

In Fig. 5, the light ray travels from the flash through the glass to the ball surface. The light is reflected by the ball surface, then through the glass again to the focus point of the camera. The angle θ_1 is defined as the angle of the light ray to the camera focus point, θ_2 as the angle of the light ray from the flash and α as the angle of the normal surface of reflection at the ball surface. The fixing ring thickness is T_f, and that of the glass is T_g. f is the distance between camera and *image plane* and r_f is the distance between camera focus point and flash.

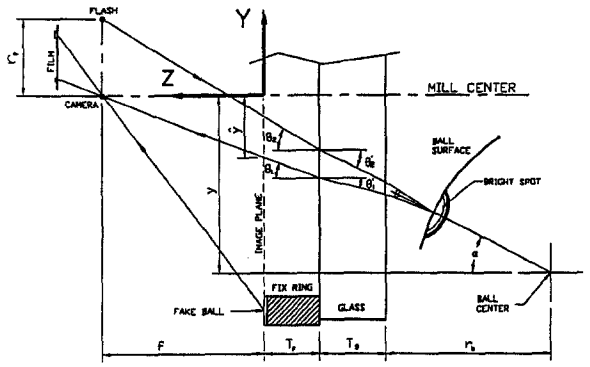

Fig. 5—Finding the *true* ball position from a ray-tracing rule

θ_1' is the angle of the refracted ray in the glass. If the refractive index of glass is n, then

$$n = \frac{\sin\theta_1}{\sin\theta_1'} \tag{6}$$

Similarly, θ_2' can be defined from

$$n = \frac{\sin\theta_2}{\sin\theta_2'} \tag{7}$$

Considering all the variables, $\hat{y}$ is the ball position found by the previous step so θ_1 can be calculated from $\theta_1 = \tan^{-1}(f / \hat{y})$. T_f, T_g, f, r_f and the ball radius r_b can be measured directly on site. This leaves three variables to be determined: θ_2, α and y.

To solve three unknowns, three independent equations are needed. Two equations can be derived from the path of the light ray in the y-direction. One is the path from the flash to the ball surface:

$$y + r_f = (f + T_f)\tan\theta_2 + T_g\theta_2' + r_b(1 - \cos\alpha)\tan\theta_2 + r_b\cos\alpha \tag{8}$$

and the other is that from the ball surface to the camera focus point:

$$y = (f + T_f)\tan\theta_1 + T_g\tan\theta_1' + r_b(1 - \cos\alpha)\tan\theta_1\, r_b\cos\alpha \tag{9}$$

The third equation is derived from the law of reflection. When the light beam strikes the surface of the ball, the angle of incidence is equal to the angle of reflection:

$$\theta_1 - \alpha = \alpha - \theta_2 \tag{10}$$

The three equations (8) through (10) are solved for the three unknowns θ_2, α and y, the true position of the ball in the y-direction.

Matching

According to the rule of matching in the second section, the matching process simply amounts to finding the nearest ball between image pairs after all the ball positions have been found. The ball distance between two images is checked and the pair of balls with the shortest distance is defined as a corresponding ball pair.

Under the constraint of eq (4) and carefully choosing the value of Δt, the matching processes are nearly always successful. There are, of course, a few unsuccessful cases which are caused by (1) incorrect ball positions and (2) irregular motion of balls due to the liner shape. As stated in the Real Ball section, it is still possible to have a few incorrect balls. When the matching fails, the positions of the balls are first rechecked. If the balls are mismatched due to their incorrect positions, the positions of the balls have to be corrected and the matching process has to be rerun. Therefore, matching can also be regarded as a confirmation procedure of the ball positions. In the second unsuccessful situation, there are always very few balls involved. They can be corrected manually by editing the list of matched balls and changing Δt in the future for that particular kind of liner.

Experimental Results and Error Estimation

Examples of the velocity fields measured by the procedure are shown in Fig. 6 for the case of the experimental ball mill with flat liner rotated at 60 percent, 70 percent, 80 percent and 90 percent of critical mill speed. The mill contains 187 30-mm diameter balls, which amounts to 30-percent filling. In Fig. 6, the small circles represent the balls which are at the corresponding positions. Short straight lines originating from the center of each small circle represent the ball velocities. A scale of magnitude of the velocity is located at the lower right-hand corner of each figure.

In Fig. 6, the balls in the outer row overlap the liner because the experimental ball mill is not perfect. This is due to wear of balls and liner, manufacturing tolerance and the eccentricity between rotation center and mill center.

The precision of measurement can be estimated by measuring the apparent velocity of static balls. The ball velocities are measured by our procedure in a stationary mill. The measurement results are expected to be zero, and therefore the nonzero results yield the measurement error.

Figure 7 shows a typical result of static ball measurement. The number inside each circle is the magnitude of the ball displacement between images in millimeters (mm). Approximately 70 percent of the balls have displacements below or near 1 mm. The scale of images with respect to the size of the experimental ball mill in our experiment is approximately 2.7 mm/pixel in the x-direction and 1.9 mm/pixel in the y-direction. The error is thus lower than the resolution of the image. Higher resolution images have been tested, but no improvement in the precision was obtained. At this point, it should be remembered that the ball locations are obtained from the center of mass of the "islands" representing the bright spots of the balls.

Since, for the experiment at 60 percent of critical mill speed, the time interval Δt was set to 7 ms and the velocity calculated by eq (3) was 1.302 m/s, the ball displacement near the liner was equal to 9.114 mm. Therefore, the relative precision on the velocity is approximately 11 percent for the balls near the liner.

The errors are caused by the following:

1. Color filters are not ideal filters so they are not identical in light transmission properties.
2. The balls are made of cast iron so their surfaces are not perfectly spherical.

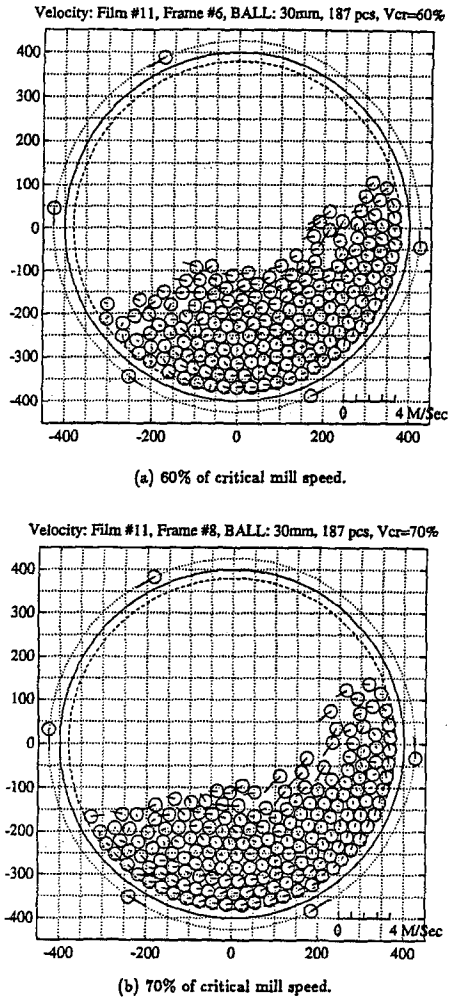

(a) 60% of critical mill speed.

(b) 70% of critical mill speed.

Fig. 6—Velocity field of flat liner at different mill speeds. (a) 60 percent of critical mill speed.

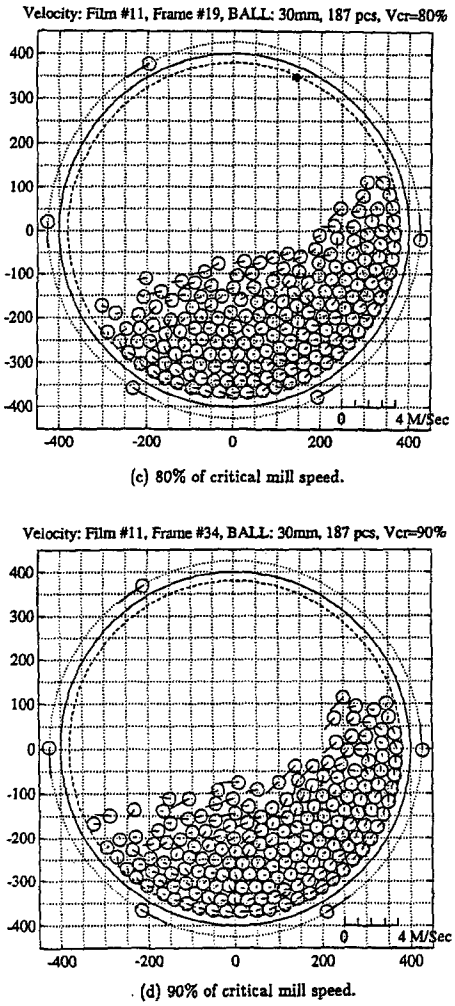

(c) 80% of critical mill speed.

(d) 90% of critical mill speed.

Fig. 6—(b) 70 percent of critical mill speed. (c) 80 percent of critical mill speed. (d) 90 percent of critical mill speed

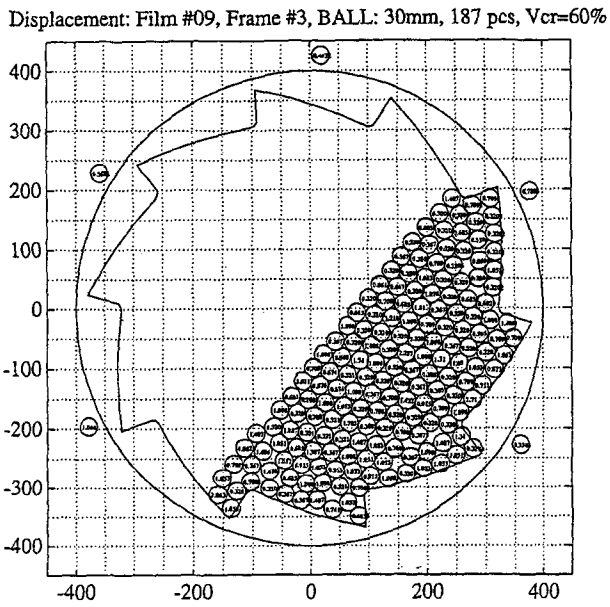

Fig. 7—Measurement error (the numbers quoted are not significant beyond 0.1 mm)

3. Lighting conditions are not homogeneous over the scene.

It is worth noting that the color filters are not ideal. When two light spots with different colors are close to each other, the ability of the filter to separate them is weaker than when the light spots are sufficiently far apart. The error estimation is measuring the distance between light spots which are very close to each other; thus it is in the worst possible situation.

Conclusion

A procedure for measuring the velocity field in a ball mill is described in this paper. The relative precision of the velocity is about 11 percent for the balls near the liner, according to the error estimation.

The following are the reasons for the measurement error.

1. The balls used in the experimental mill are produced by casting, so the ball surface is not perfectly spherical. Machined balls (e.g., bearing balls) could improve the precision of measurement.

2. The glass shield is not perfectly flat due to the fixing bolts, therefore the image is distorted.

3. The properties of color filters are not identical. Good quality color filters are desirable.

4. A very simple matching process is used. If the matching process added more constraints during the search for the nearest ball, then Δt could be increased, and the relative precision could be accordingly improved.

In the measurement procedure, setting the Δt of two successive images is critical to both the measurement precision and the matching process. For a precise instantaneous velocity, Δt should approach zero. But, in practice, the precision of the measurement is already determined by the resolution of an image. The measurement error will be increased if we decrease Δt. Nor can Δt be too large, since it increases Δd and makes the matching process difficult. Consequently, a trade-off is necessary in setting Δt.

The velocity field of a ball mill can be used to evaluate the performance of a mill liner. For example, the velocity difference between the outer row balls and the liner gives a quantitative idea of the sliding between the load and the liner. Also, the velocity of a free-flying ball can tell about the launch and the impact point of the ball. The liner design can thus be improved by examining the velocity field.

This procedure could be further developed in order to find accelerations of the balls by taking three successive images, $I_{t-\Delta t}$, I_t and $I_{t+\Delta t}$, using three flashes with three complementary colors. Since the acceleration involves one additional time derivative, the error of acceleration measurement will be greater than that of velocity measurement. In such an extension, therefore, one must be aware of the possible errors involved.

Appendix

The Laplacian operator[4] is an approximation to the equation

$$\frac{\delta^2 E}{\delta x^2} + \frac{\delta^2 E}{\delta y^2}$$

where E is the image brightness. The corresponding stencil is

$$\begin{bmatrix} 0 & -1 & 0 \\ -1 & 4 & -1 \\ 0 & -1 & 0 \end{bmatrix}$$

Since each pixel intensity is recalculated as four times its own value, minus each of its nearest neighbors, this operator enhances the image of a spherelike surface having rotational symmetry. Cylindrical or flat surfaces will disappear after applying this operator.

Acknowledgments

This research is supported by S.A. Slegten (member of Magotteaux Group), Belgium. The authors would like to thank Mr. Werbrouck who initiated this project and Mr. Thomart who supported us thereafter. Our thanks to M. Dewan for designing the control device and K. Lipinski for giving us the idea of using different color images.

References

1. Aggarwal, J.K. and Nandhakumar, N., "On the Computation of Motion from Sequences of Images—A Review," Proc. IEEE, **76** *(8), 917–935 (August 1988).*

2. Bhanu, B., Nevatia, R. and Riseman, E.M., "Dynamic-scene and Motion Analysis Using Passive Sensors, Part II: Displacement-field and Feature-based Approaches," IEEE Expert, 53–64 (February 1992).

3. Dunn, D.J. and Martin, R.G., "Measurement of Impact Forces in Ball Mills," Min. Eng., 384–388 (April 1978).

4. Horn, B.K.P., Robot Vision, MIT Press, Cambridge, MA, Ch. 8, 161–184 (1987).

5. Lukasiewicz, S.A., Swisterski, W. and Romaniszyn, G., "Supercritical Revolutions of Tumbling Mills," Minerals & Metallurgical Processing, 100–106 (May 1990).

6. McIvor, R.E., "Effects of Speed and Liner Configuration on Ball Mill Performance," Min. Eng., 617–622 (January 1985).

7. Mishra, B.K. and Rajamani, R.K., "Numerical Simulation of Charge Motion in Ball Mills—Lifter Bar Effects," Paper presented at the SME Annual Meeting, Phoenix, AZ (February 24-27, 1992).

8. PC-SCOPE Manuel d'Utilisation IDS542, Version 3.0, i2S, Bordeaux, France (1989).

9. Vermeulen, L.A., "The Lifting Action of Lifter Bars in Rotary Mills," J. South Afr. Inst. Min. Metall., **85** *(2), 41–49 (February 1985).*